# LOCALIZED SINGULAR BOUNDARY METHOD FOR SOLVING THE CONVECTION–DIFFUSION EQUATION WITH VARIABLE VELOCITY FIELD

JURAJ MUŽÍK & ROMAN BULKO
Department of Geotechnics, University of Žilina, Slovakia

ABSTRACT
This paper focuses on deriving the local variant of the singular boundary method (SBM) to solve the convection–diffusion equation. Adopting the combination of an SBM and finite collocation, one obtains the localized variant of SBM. Unlike the global variant, local SBM leads to a sparse matrix of the resulting system of equations, making it much more efficient to solve large-scale tasks. It also allows solving velocity vector variable tasks, which is a problem with global SBM. The article presents the steady numerical example for the convection–diffusion problem with variable velocity field and examines the dependence of the accuracy of the solution on the nodal grid's density and the subdomain's size.
*Keywords: singular boundary method, finite collocation, convection–diffusion.*

## 1 INTRODUCTION

Methods based on the theory of boundary integrals are an essential group of numerical methods used in engineering practice. The original boundary integral and boundary element method (BEM) [1] are currently complemented by the fundamental solution method (MFS) [2] and, more recently, the boundary node method (BNM) [3] or the singular boundary method (SBM) [4]. The indirect formulation of the boundary integral serves as the base for the MFS and SBM methods. In contrast to direct formulations, where the primary variable is the value of the searched function, indirect formulations first look for a set of coefficients to evaluate the solution. The global nature of these methods indicates that a solution at an arbitrary location within the computational domain uses the global boundary values and results in a fully populated and often poorly conditioned equation system, especially in large 3D systems. This problem is currently most often solved by dividing the original area into smaller non-overlapping sub-domains (DRMMD [5] or SBMMD methods [6]). Initially, these methods have been successfully used primarily to address the non-homogeneity of the area and are suitable for large scale treatment of the resulting matrices. The main drawback of this approach is the increase in the number of equations caused by the necessary compatibility equations at the boundary of the subdomain. The promising principle of finite collocation (FC), as formulated by Stevens et al. [7], showed the potential to formulate indirect methods locally without a need to create and manage subdomains [8]. Like other local methods, the method defines a set of simple overlapping subdomains around the points at which the solution of the corresponding partial differential equation (PDE) is evaluated. However, unlike other conventional schemes, it uses only the boundary points of that subdomain for this local solution. This approach results in a sparse global system of linear equations to obtain the solution at all interior points. The article focuses on the solution to the steady convection–diffusion problem with a variable velocity field.

## 2 NUMERICAL SOLUTION

The localization of the global SBM is realized by adopting the finite collocation approach [8]. The set of points covers the computational domain $\Omega$ with global boundary $\Gamma$, and the

WIT Transactions on Engineering Sciences, Vol 134, © 2022 WIT Press
www.witpress.com, ISSN 1743-3533 (on-line)
doi:10.2495/BE450101

neighbouring nodes create the local domain around each node (Fig. 1) – the domain centre. The points that form the local domain boundary represent the local model used to evaluate the solution in the domain centres. The local model boundary values are assumed to be part of the solution except for the nodes that belong to the global boundary.

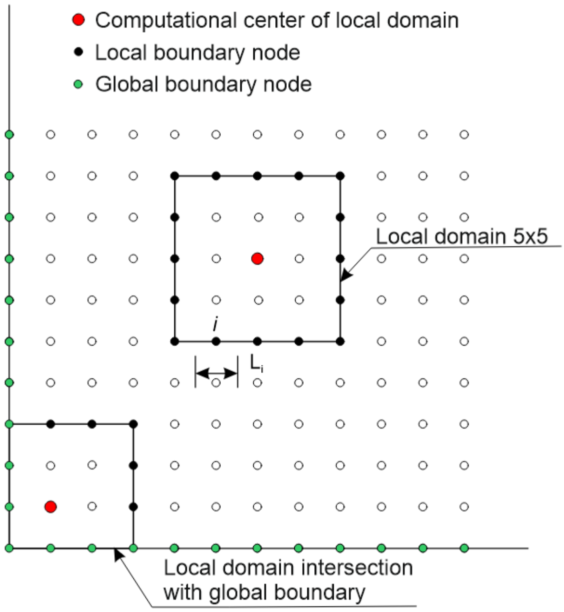


Figure 1: SBM models for local domains.

### 2.1 Governing equations

The problem being considered is described by the steady convection–diffusion differential equation [9]:

$$D\Delta C(\mathbf{x}) - \mathbf{v} \cdot \nabla C(\mathbf{x}) - \lambda \nabla C(\mathbf{x}) = 0 \quad \mathbf{x} \in \Omega, \tag{1}$$

where $C$ is the concentration of the tracer, $D$ is the coefficient of dispersion, $\lambda$ is the decay constant, $\mathbf{v}$ is the velocity vector field, and $\mathbf{x}$ is the spatial coordinate vector. The Dirichlet and Neumann boundary conditions (BC) need to be specified to solve the governing equation. The Dirichlet BC specifies the value of the tracer concentration $C$ on the part of boundary $\Gamma_1$, and the Neumann BC gives the flux $q_0$ with concentration $C_0$ perpendicular to the boundary $\Gamma_2$.

### 2.2 Localized singular boundary method

The local model for each local subdomain is formulated adopting the singular boundary method (SBM). Expressing SBM solution at each local domain centre, assuming unknown boundary values, creates a set of local SBM systems

$$\sum_{j=1}^{n} \mathrm{A}_{ij}^{k}\, \alpha_j^k = d_i^k \qquad k = 1,2,\dots,N, \tag{2}$$

where $n$ is the number of boundary nodes in the local subdomain $k$. The elements of matrix **A** are expressed as follows

$$\mathrm{A}_{ij}^{k} = G^{k}(r_{ij}) \quad i \neq j, \ \mathrm{A}_{ii}^{k} = U_{ii}^{k} \quad i = j, \tag{3}$$

where $G^{k}(r_{ij})$ is the fundamental solution of eqn (1) and $r_{ij}$ is the distance between boundary nodes of the local SBM model. If $i$=$j$, the fundamental solution is singular and the origin intensity factor (OIF) $U_{ii}^{k}$ is used instead [10]. The fundamental solution of the convection–diffusion equation is [11]

$$G^{k}(r_{ij}) = \frac{1}{2\pi D} e^{\left(-\frac{\mathbf{v}\cdot\mathbf{r}}{2D}\right)} K_0(\mu r_{ij}), \tag{4}$$

where $K_0$ is the Bessel function of the second kind of order zero and

$$\mu = \sqrt{\left(\frac{|v|}{2D}\right)^2 + \frac{\lambda}{D}}. \tag{5}$$

The Dirichlet origin intensity factor $U_{ii}$ can be evaluated using a similar procedure as in Chen et al. [12]

$$U_{ii} = \frac{1}{2\pi D}\left[ln\left(\frac{L_i}{2\pi}\right) - ln\left(\frac{\mu}{2}\right) - \gamma\right], \tag{6}$$

where $L_i$ is the length of the local domain boundary part under influence of point $i$ (see Fig. 1) and $\gamma$ is the Euler constant.

The values $\alpha_j^k$ are the interpolation coefficients for local domain $k$. The vector $d_i^k$ on the right side of eqn (2) contains the unknown solution value in solution centres on the local domain $k$. The solution in the centre point $x_c$ of the local domain $k$ can be expressed as

$$C^{k}(x_c) = \sum_{j=1}^{n} G^{k}(r_{cj})\alpha_j^k, \tag{7}$$

where $r_{cj}$ is the distance between the centre point $x_c$ and the local boundary node $j$. From eqn (3), the vector $\alpha$ can be expressed as

$$\alpha^k = \left(\mathbf{A}^k\right)^{-1}\mathbf{d}^k. \tag{8}$$

If we substitute eqn (8) into eqn (7) we get

$$C^{k}(x_c) = \sum_{j=1}^{n} \mathbf{G}_c^k\left(\mathbf{A}^k\right)^{-1}\mathbf{d}^k = \mathbf{W}_c^k\mathbf{d}^k, \tag{9}$$

where $\mathbf{W}_c^k$ is a local domain weight vector [7] which can be used to create the global system of equations. This system is sparse and can be defined as

$$\mathrm{C}_k - \sum_{j=1}^{n} \mathrm{W}_j^k\,\mathrm{C}_j = \sum_{l=1}^{m} \mathrm{W}_l^k b_{ol}, \tag{10}$$

where $n$ is the number of local boundary nodes and $m$ is the number of global boundary centres for the $k$th local domain. The system of $N$ sparse linear equations is formed. We can solve these $N$ equations to obtain solution values at all internal nodes.

## 3 NUMERICAL EXAMPLE: STEADY CASE WITH VARIABLE VELOCITY

This example is very often used as a test of different implementations of BEM and DRM methods [9], [13]. The horizontal velocity is a function of $x$-coordinate and a decay constant $\lambda$. Though the analytical solution is independent of the $y$-coordinate, from the numerical scheme point of view the solution is a 2D one since the code needs to accurately predict that in the $y$-coordinate, the solution is constant for a given spatial position, and also that the side flux is zero. This example is challenging to solve because the velocity changes direction inside the solution domain. The velocity field is expressed as

$$v_x = ln\left(\frac{C_1}{C_0}\right) + \lambda\left(x - \frac{1}{2}\right). \tag{11}$$

The rectangular domain [0, 1]×[0, 0.2] has been used with Dirichlet boundary conditions $C(0, y) = C_0 = 300$, $C(1, y) = C_1 = 10$, Neumann boundary conditions $q(x, 0) = q(x, 0.2) = 0$, and dispersion coefficient $D = 1$. Then the exact solution can be written as

$$C(x) = C_0 e^{\left[\lambda\frac{x^2}{2} + x\left(ln\left(\frac{C_1}{C_0}\right) - \frac{\lambda}{2}\right)\right]}. \tag{12}$$

Two different values of the decay constant $\lambda$ have been considered, $\lambda = 10$, and $\lambda = 40$. The solutions obtained for described boundary conditions are visualized in Figs 4, 5 and 6, with the effect of local domain size. Fig 2, 3, 7 and 8 show the relative error rates as a percentage for different local domain sizes on two computational grids (51×11 and 81×21 points). The optimal dimension of the local domain depends on the values of $\lambda$ for this particular problem. While for $\lambda = 10$ with increasing size decreases relative error, the value $\lambda = 40$ the effect is opposite. The velocity gradient most likely causes this behaviour. It is considerably higher for $\lambda = 40$, and the larger dimension of the local domain cannot model these changes adequately. Table 1 shows the solution values and relative error distribution multiple domain dual reciprocity method (DRMMD) [13], radial boundary integral equation method (RBIEM) [9] and the present LSB method. The LSBM results are comparable with DRMMD for the optimal size of the local domain.

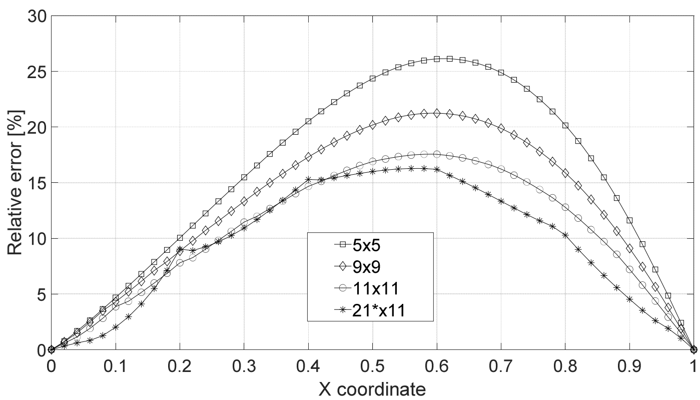


Figure 2: Relative errors for various local subdomain sizes: $\lambda = 10$, grid of 51×11 nodes.

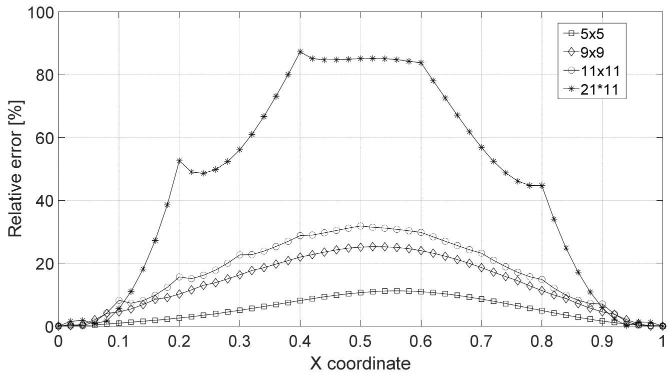


Figure 3: Relative errors for various local subdomain sizes: λ = 40, grid of 51×11 nodes.

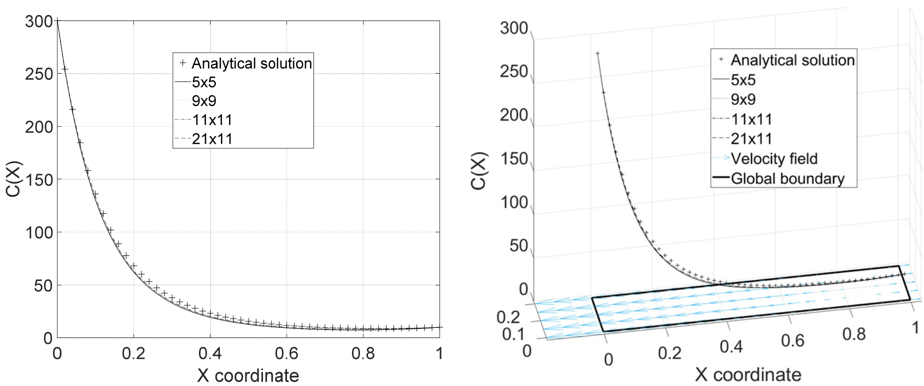


Figure 4: Concentration solution for λ = 10, and comparison of various local subdomain sizes with the analytical solution for grid 51×11 nodes.

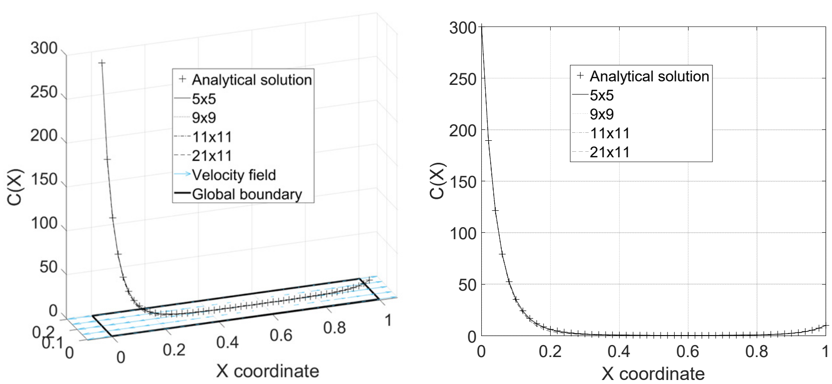


Figure 5: Concentration solution for λ = 40, and comparison of various local subdomain sizes with the analytical solution for grid 51×11 nodes.

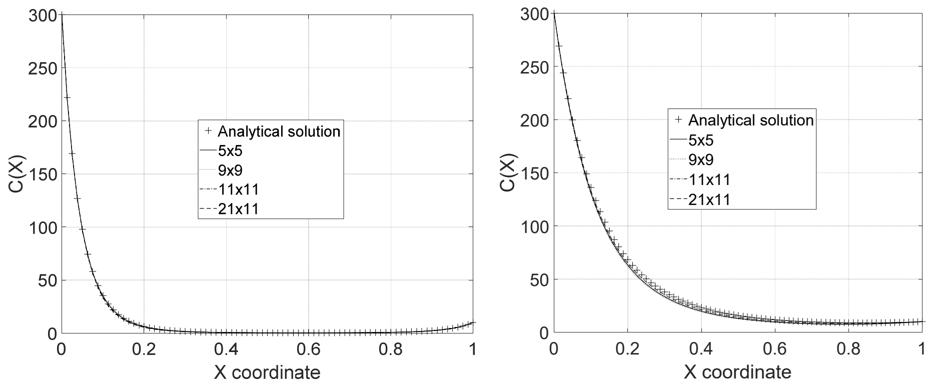


Figure 6: Concentration solution for λ = 40 (left) and λ = 10 (right), and comparison of various local subdomain sizes with the analytical solution for grid 81×21 nodes.

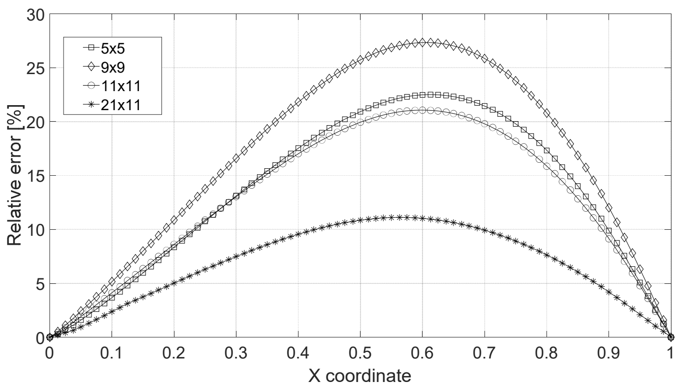


Figure 7: Relative errors for various local subdomain sizes: λ = 10, a grid of 81×21 nodes.

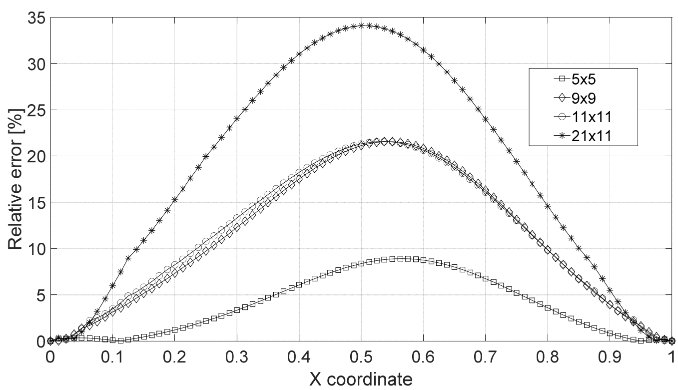


Figure 8: Relative errors for various local subdomain sizes: λ = 40, a grid of 81×21 nodes.

Table 1: Comparison of the results for concentration obtained using the LSBM compared with the analytical solution and results of RBIEM, DRMMD for a regularly distributed 81×21 nodes (case k = 40).

| X | Analytical solution | LSBM 5×5 | RBIEM | DRMMD | LSBM error (%) | RBIEM error (%) | DRMMD error (%) |
|---|---|---|---|---|---|---|---|
| 0.00 | 300.000 | 300.000 | 300.000 | 300.000 | 0.000 | 0.000 | 0.000 |
| 0.02 | 189.380 | 190.724 | 179.046 | 187.617 | 0.271 | 5.456 | 0.930 |
| 0.04 | 121.478 | 121.636 | 118.357 | 118.989 | 0.351 | 2.569 | 2.048 |
| 0.07 | 64.308 | 64.658 | 63.181 | 62.420 | 0.278 | 1.753 | 2.936 |
| 0.10 | 35.292 | 35.264 | 35.161 | 34.329 | 0.080 | 0.371 | 2.728 |
| 0.14 | 16.770 | 16.775 | 17.055 | 16.689 | 0.324 | 1.697 | 0.485 |
| 0.19 | 7.239 | 7.185 | 7.470 | 7.609 | 1.030 | 3.191 | 5.104 |
| 0.25 | 3.014 | 2.950 | 3.146 | 3.449 | 2.166 | 4.367 | 14.416 |
| 0.32 | 1.301 | 1.256 | 1.349 | 1.633 | 3.852 | 3.690 | 25.545 |
| 0.40 | 0.633 | 0.597 | 0.662 | 0.850 | 6.078 | 4.603 | 34.335 |
| 0.56 | 0.323 | 0.297 | 0.347 | 0.437 | 8.894 | 7.387 | 35.252 |
| 0.75 | 0.550 | 0.523 | 0.594 | 0.690 | 5.204 | 8.099 | 25.478 |
| 0.85 | 1.300 | 1.274 | 1.329 | 1.568 | 2.078 | 2.247 | 20.633 |
| 0.93 | 3.451 | 3.458 | 3.280 | 3.923 | 0.272 | 4.943 | 13.701 |
| 1.00 | 10.000 | 10.000 | 10.000 | 10.000 | 0.000 | 0.000 | 0.000 |

## 4 CONCLUSIONS

This paper focused on the possibility of localization of the singular boundary method in solving both the steady convection–diffusion equations with the possibility of decay of the tracer and variable velocity field. The localization of SBM was achieved by adopting the principles of the finite collocation method. Test numerical examples showed the resulting combination of these two methods as promising alternatives to multi-domain methods, even for cases with a non-uniform velocity field.

## ACKNOWLEDGEMENT

This contribution is the result of the project funded by the Scientific Grant Agency of Slovak Republic (VEGA) No. 1-0879-21.

## REFERENCES

[1] Brebbia, C.A., Telles, J.C.F. & Wrobel, L.C., *Boundary Element Techniques*, Springer-Verlag: Berlin and New York, pp. 11–13, 1984.

[2] Chen, C.S., Karageorghis, A. & Li, Y., On choosing the location of the sources in the MFS. *Numerical Algorithms*, **72**, pp. 107–130, 2016.

[3] Yan, F., Yu, M. & Lv, J.H., Dual reciprocity boundary node method for convection–diffusion problems. *Engineering Analysis with Boundary Elements*, **80**, pp. 230–236, 2017.

[4] Kovářík, K., Mužík, J., Bulko, R. & Sitányiová, D., Singular boundary method using dual reciprocity for two-dimensional transient diffusion. *Engineering Analysis with Boundary Elements*, **83**, pp. 256–264, 2017.

[5] Florez, W., Power, H. & Chejne, F., Multi-domain dual reciprocity BEM approach for the Navier–Stokes system of equations. *Communications in Numerical Methods in Engineering*, **16**, pp. 671–681, 2000.
[6] Mužík, J. & Bulko, R., Multidomain singular boundary method for 2D laminar viscous flow. *WIT Transactions on Engineering Sciences*, vol. 122, WIT Press: Boston and Southampton, pp. 131–141, 2019.
[7] Stevens, D., Power, H., Meng, C.Y., Howard, D. & Cliffe, K.A., An alternative local collocation strategy for high-convergence meshless PDE solutions, using radial basis functions. *Journal of Computational Physics*, **294**, pp. 52–75, 2013.
[8] Kovářík, K., Mužík, J., Bulko, R. & Sitányiová, D., Local singular boundary method for two-dimensional steady and unsteady potential flow. *Engineering Analysis with Boundary Elements*, **108**, pp. 168–178, 2019.
[9] Popov, V. & Bui T.T., A meshless solution to two-dimensional convection–diffusion problems. *Engineering Analysis with Boundary Elements*, **34**(7), pp. 680–689, 2010.
[10] Kovářík, K., Mužík, J., Masarovičová, S. & Sitányiová, D., Regularized singular boundary method for 3D potential flow. *Engineering Analysis with Boundary Elements*, **95**, pp. 85–92, 2018.
[11] Singh, K.M. & Tanaka, M., Dual reciprocity boundary element analysis of transient advection–diffusion. *International Journal of Numerical Methods in Heat and Fluid Flow*, **13**, pp. 633–646, 2003.
[12] Chen, W., Zhang, J.Y. & Fu, Z.J., Singular boundary method for modified Helmholtz equations. *Engineering Analysis with Boundary Elements*, **44**, pp. 112–119, 2014.
[13] Bui, T.T. & Popov, V., Domain decomposition boundary element method with overlapping sub-domains. *Engineering Analysis with Boundary Elements*, **33**, pp. 456–466, 2009.